



## Article

# Influence of Reed Fiber Length and Dosage on the Properties of Reed-Fiber-Modified Bitumen and Bituminous Mortar

Huikun Chen <sup>1</sup>, Junyan Zhang <sup>2</sup>, Dongyu Niu <sup>1,\*</sup> , Xueyan Liu <sup>3</sup>  and Peng Lin <sup>4</sup>

<sup>1</sup> School of Materials Science and Engineering, Chang'an University, Xi'an 710061, China; 2022131076@chd.edu.cn

<sup>2</sup> Shaanxi Construction Engineering Eighth Construction Group Co., Ltd., Xi'an 710061, China; zachjunyan@foxmail.com

<sup>3</sup> Section of Pavement Engineering, Department of Engineering Structures, Faculty of Civil Engineering and Geosciences, Delft University of Technology, Stevinweg 1, 2628 CN Delft, The Netherlands; x.liu@tudelft.nl

<sup>4</sup> Ministry of Infrastructure and Water Management (Rijkswaterstaat), Griffioenlaan 2, 3526 LA Utrecht, The Netherlands; peng.lin@rws.nl

\* Correspondence: niudongyu\_1984@chd.edu.cn

**Abstract:** In order to explore the feasibility and efficacy of reed-fiber-modified bitumen (RFMB), three lengths and three dosages of reed fibers were selected to modify bitumen and bituminous mortar, while the physicochemical properties of RFMB and RFMB mortar were analyzed. In this work, FTIR spectroscopy was employed to characterize the chemical impact of fiber on bitumen. The viscosity and rheology of RFMB and the tensile strength of RFMB mortar were evaluated using a Brookfield viscometer, dynamic shear rheometer, and monotonic tensile test. The results showed that adding fibers primarily affects the physical structure rather than the chemical composition of bitumen, confirmed by FTIR spectroscopy. RFMB viscosity increased with higher fiber dosage and fiber length. Rheological evaluations showed an enhanced complex shear modulus for RFMB, suggesting improved performance at higher temperatures but increased stiffness at lower temperatures, with the latter indicating reduced flexibility. RFMB also demonstrated superior fatigue and rutting resistance, albeit with compromised stress sensitivity. Tensile tests on RFMB mortar highlighted significant improvements, especially with longer fibers, while shorter 0.4 mm fibers showed modest reinforcement effects, possibly due to uneven distribution during sample preparation.

**Keywords:** bitumen; reed fiber; mortar; rheological; performance characterization



**Citation:** Chen, H.; Zhang, J.; Niu, D.; Liu, X.; Lin, P. Influence of Reed Fiber Length and Dosage on the Properties of Reed-Fiber-Modified Bitumen and Bituminous Mortar. *Buildings* **2024**, *14*, 2749. <https://doi.org/10.3390/buildings14092749>

Academic Editor: Paulo Santos

Received: 23 July 2024

Revised: 16 August 2024

Accepted: 30 August 2024

Published: 2 September 2024



**Copyright:** © 2024 by the authors. Licensee MDPI, Basel, Switzerland. This article is an open access article distributed under the terms and conditions of the Creative Commons Attribution (CC BY) license (<https://creativecommons.org/licenses/by/4.0/>).

## 1. Introduction

Bitumen is the cornerstone of road pavement construction worldwide, and is crucial for creating resilient and durable road surfaces. The increasing volume of traffic and the diverse environmental conditions to which roads are exposed demand enhanced performance from bitumen. Traditional bitumen often struggles to meet these rigorous requirements, including varying climate conditions, heavy traffic loads, and evolving pavement structures. Consequently, modifying bitumen has emerged as a crucial strategy to improve its performance, durability, and adaptability under challenging conditions [1].

Historically, the enhancement of bitumen has largely relied on synthetic polymers. These polymers improve various bitumen properties, such as flexibility, resistance to deformation, and temperature susceptibility. However, with the growing emphasis on sustainability and eco-friendly construction practices, there is a rising interest in natural and renewable alternatives. Natural fibers, including reed fibers, have garnered attention as promising additives that can not only reinforce bitumen but also align with sustainable construction goals [2–4].

Research into fiber-modified bitumen has demonstrated various benefits. For instance, fibers such as glass and metal have been shown to enhance bitumen's resistance to thermal deformation and rutting [5]. Cellulose fibers have been effective in improving the

performance of recycled bitumen concrete by increasing its rutting resistance and moisture stability [6].

Amidst this backdrop, reed fibers have emerged as a promising candidate due to their widespread availability and renewable nature. Reed, thriving in wetland environments globally except Antarctica, offers advantages such as rapid growth and resilience to frequent cutting without the need for fertilizers. Moreover, reed cultivation can contribute to environmental conservation efforts by preventing peatland drainage, thereby mitigating greenhouse gas emissions [7,8].

Reed fibers, known for their high lignin content, mechanical strength, and rapid growth, present a compelling alternative to synthetic fibers. They have been successfully utilized in other applications such as insulation panels and composite materials, where they enhance mechanical and thermal properties [9–12].

Despite these advances, there is a notable gap in the literature regarding the specific effects of fiber length and dosage on bitumen properties. Most existing studies have focused on general benefits rather than a detailed examination of how varying fiber dimensions and concentrations affect bitumen's performance.

Bituminous mortar, which integrates bitumen with aggregates, plays a critical role in road construction by providing necessary structural support and durability. Although previous research has explored the impact of various modifiers on bituminous mortar, there is limited understanding of how different fiber lengths and dosages influence its properties [13]. This gap is particularly evident with natural fibers like reed, which have not been extensively studied in the context of bituminous mortar.

This study aims to bridge this gap by investigating the impact of reed fibers on bitumen. Specifically, we will explore how varying fiber lengths (<0.4 mm, 0.4–0.6 mm, and 0.8 mm) and dosages (2%, 6%, and 10%) affect the properties of reed–fiber-modified bitumen (RFMB). Through a comprehensive series of tests, including viscosity, frequency sweep, multiple stress creep recovery, linear amplitude sweep, and monotonic tensile tests, this research will provide valuable insights into optimizing reed fibers for bituminous mortar.

## 2. Materials and Methods

### 2.1. Raw Materials

#### 2.1.1. Base Bitumen

The experiments utilized a 70/100 bitumen binder from Total Nederland N.V. (Den Haag, The Netherlands). Table 1 presents the physical properties and chemical components of this bitumen binder. In Table 1, The Asphaltene Colloidal Index (AsColloidal Index, CI) is a key parameter used to evaluate the colloidal stability of asphaltenes within bitumen. This index provides valuable information regarding the dispersion and interactions of asphaltenes with other bitumen constituents, thereby influencing the overall performance and rheological properties of the bitumen.

**Table 1.** Physical properties and chemical components of virgin bitumen.

Properties	Value	Test Standard
25 °C Penetration (1/10 mm)	91	ASTM D5 [14]
Softening point (°C)	48	ASTM D36 [15]
135 °C Dynamic viscosity (Pa·s)	0.8	AASHTO T316 [16]
25 °C Density	1.017	EN 15326 [17]
60 °C Density	0.996	
Chemical fractions (wt %)	Saturate, S	3.6
	Aromatic, A	53.3
	Resin, R	30.3
	Asphaltene, AsColloidal Index CI	12.8

Table 1. Cont.

Properties		Value	Test Standard
Element compositions	Carbon, C	84.06	ASTM D7343 [19]
	Hydrogen, H	10.91	
	Oxygen, O	0.62	
	Sulphur, S	3.52	
	Nitrogen, N	0.9	
Complex shear modulus at 1.6 Hz and 60 °C (kPa)		2.4	AASHTO M320 [20]
Phase angle at 1.6 Hz (°)		84.5	

### 2.1.2. Reed Fiber

The reed fibers of varying lengths were sourced from ESEM, Eindhoven, The Netherlands. These fibers, characterized by a golden hue and dry texture, retained their natural surface without modification.

In this study, we selected specific reed fiber lengths and dosages based on practical and experimental considerations. The fiber lengths chosen were <0.4 mm, 0.4–0.6 mm, and 0.8 mm. Fibers shorter than 0.4 mm tend to provide insufficient reinforcement, while fibers longer than 0.8 mm can intertwine, complicating blending with bitumen and causing “balling” issues [21]. The intermediate lengths of 0.4–0.6 mm were included to assess their effectiveness relative to the extremes. According to preliminary investigation results, we excluded the 0.6–0.8 mm length group due to similar performance results observed with 0.8 mm fibers.

In this research, the impact of reed fiber length on bituminous binder was investigated. Four lengths of reed fibers (<0.4 mm, 0.4–0.6 mm, 0.6–0.8 mm, 0.8 mm) were selected, as depicted in Figure 1. Fibers that are excessively long may intertwine, posing challenges in blending with bitumen and causing “balling” issues. Conversely, fibers that are too short provide inadequate reinforcement, making their inclusion as a filler futile and costly [22].



Figure 1. Appearance of reed fiber (0.8 mm, 0.6 mm to 0.8 mm, 0.4 mm to 0.6 mm, and less than 0.4 mm).

The reed fibers were mixed with bitumen at specified ratios based on bitumen mass. High-, medium-, and low-fiber dosages—referenced from experimental doses of corn stalk fibers with properties similar to reed fibers [22]—were set at 2%, 6%, and 10%. Following previous experimental findings that revealed negligible performance differences between 0.6–0.8-millimeter-diameter fibers and 0.8 mm fibers, the 0.6–0.8 mm group was excluded from subsequent experiments. The physical and mechanical properties of the reed fiber are shown in Table 2.

Table 2. Physical and mechanical properties of the reed fiber.

Property	Density	Tensile Strength	Elastic Modulus	Lignin Content	Moisture Content
Range	1.1~1.2 g/cm <sup>3</sup>	30~70 MPa	2.5~4.5 GPa	20~30%	10~15%

## 2.2. Preparation of the Modified Bitumen

To mitigate the potential impact of high-speed shearing on fiber length, a method involving low-speed agitation was employed. Following the procedures used for preparing other fiber-modified bitumen of similar structure [23,24], the preparation of RFMB proceeded as follows:

- (1) The reed fibers were weighed according to specified dosages based on the weight of the bitumen;
- (2) The bitumen and fibers were combined and placed in an oven, where they were heated to 150 °C;
- (3) Subsequently, the heated mixture was gradually introduced into the bitumen and blended at low speed for 30 min to achieve even dispersion of the fibers.

Refer to Figure 2 for a visual representation of the RFMB preparation process.

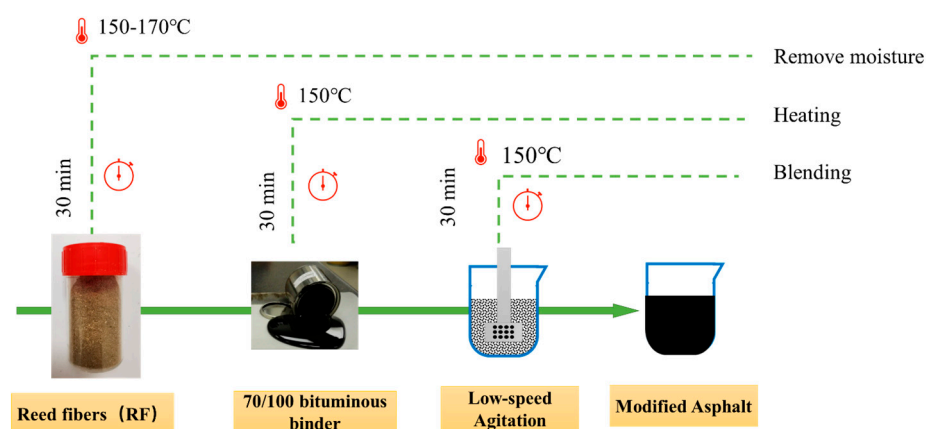


**Figure 2.** Process of preparing reed-fiber-modified bituminous binder.

## 2.3. Test Methods

### 2.3.1. Fourier-Transform Infrared Spectroscopy (FTIR)

FTIR was employed to investigate the effects of reed fibers on the modified binder. The fibers were added at different weights (2%, 6%, and 10%). This analysis aimed to determine any alterations in the chemical structure of the bitumen resulting from the fiber additions. The FTIR device used for this analysis was from Waltham, MA, USA, which provided precise spectral data to identify and quantify the chemical changes induced by the incorporation of reed fibers. The procedure followed was outlined in ASTM E1252-98 [25].

### 2.3.2. Viscosity

The viscosity of the reed-fiber-modified bitumen was tested using fibers of three different lengths (<0.4 mm, 0.4–0.6 mm, and 0.8 mm) and varying dosages (2%, 6%, and 10%). Viscosity serves as a critical indicator of bitumen's flow characteristics and workability during construction. Following standard rotational viscosity test procedures, viscosity measurements were conducted at different temperatures using a Brookfield viscometer (Changji Geological Instrument CO., Ltd., Shanghai, China), adhering to ASTM D4402-14 [26].

### 2.3.3. Rheological Measurements

This section uses the SmartPave 102 DSR (SmartTest, Uppsala, Sweden) testing device to evaluate the rheological performance of reed-fiber-modified bitumen.

#### (1) Frequency Sweep

Complex modulus and phase angle measurements were conducted on reed-fiber-modified bituminous binder across various temperatures (0 °C, 15 °C, 30 °C, 40 °C, 60 °C, and 80 °C) and frequencies (0.1–10 Hz). Master curves were then constructed to represent the collected data. The time–temperature superposition principle was used to create a master curve for modified bitumen, with 30 °C as the reference temperature. Fitting



parameters for the complex modulus were then determined based on this model [27]. Fitting parameters were derived as per ASTM D7175-15 [28].

$$\lg|G^*| = \delta + \frac{\alpha}{1 + e^{\beta + \gamma \times \lg(f_r)}} \quad (1)$$

where  $G^*$  represents the complex modulus;  $\delta$  denotes the lower asymptote of complex shear modulus  $|G^*|$ ;  $\alpha$  denotes the upper asymptote of the complex shear modulus  $|G^*|$ ;  $\beta$  and  $\gamma$  are the shape factors.

#### (2) Multiple stress creep recovery (MSCR)

The MSCR method outlined in ASTM D7405-15 [29] identified the elastic response of bitumen and its variation under two different stress levels. This study aimed to evaluate the impact of reed fiber addition on rutting resistance through analysis of parameters including percentage recovery and non-recoverable creep flexibility of the bitumen.

#### (3) Relaxation test

Bitumen samples were analyzed using a DSR equipped with an 8-millimeter-diameter plate and a 2 mm gap at a temperature of 0 °C. The relaxation tests began with a 1% shear strain applied over 0.1 s, followed by a 100-s relaxation period. Data were collected at a frequency of 100 Hz, following the protocol in ASTM D7316-15 [30]. These tests are essential for evaluating the stress generation and relaxation capabilities of bitumen at low temperatures.

#### (4) Linear Amplitude Sweep (LAS)

An LAS test was conducted to evaluate fatigue criteria. Initially, a frequency sweep assessed rheological properties by applying a constant 0.1% strain across frequencies ranging from 0.2 to 30 Hz, with data used to determine the “alpha” parameter for damage analysis.

Following this, at a consistent 10 Hz frequency, the LAS test involved incrementally increasing strain from zero to 30% over 3100 cycles to simulate accelerated fatigue damage. Key metrics such as peak shear strain, peak shear stress, phase angle, and dynamic shear modulus were recorded at 10-cycle intervals, as detailed in ASTM D7405-15.

These tests provide comprehensive insights into the material’s fatigue behavior under varying strain amplitudes and frequencies, critical for understanding its durability and performance characteristics.

### 2.3.4. Monotonic Tensile Testing of Mortar Reinforced with Reed Fibers

In the context of fatigue and crack resistance, the tensile strength of bituminous mixtures plays a critical role. Traditional uniaxial direct tensile testing of cylindrical samples often encounters challenges, such as uncertain failure locations, particularly near the specimen’s end caps [31]. To ensure controlled tensile failure at the specimen’s center, a complex dog-bone-shaped geometry was adopted [32]. This study aimed to investigate the impact of reed fibers on the mechanical properties of bitumen mortar specimens, which were shaped into a parabolic form with a central straight section.

The test specimens were prepared using a systematic procedure: Bitumen, sand, and fibers were initially heated to the specified temperature and mixed in proportions outlined in Table 3 to form the mortar mixture. The mixture was then reheated in an oven to maintain its rheological properties and facilitate handling. Concurrently, a silicone mold was also preheated. The mortar was poured into the heated mold (see Figure 3a), allowed to settle briefly to fill any voids, and then transferred to a refrigerator. Cooling in the refrigerator stiffened the samples, facilitating easy demolding while retaining their shape. The properties of the sand used in bituminous mortar are shown in Table 4.

**Table 3.** Material dosage per set of three prepared specimens.

Species	Sand	Bitumen	Filler	Reed Fiber		
				2%	6%	10%
Dosage	100 g	50 g	50 g	1 g	3 g	5 g

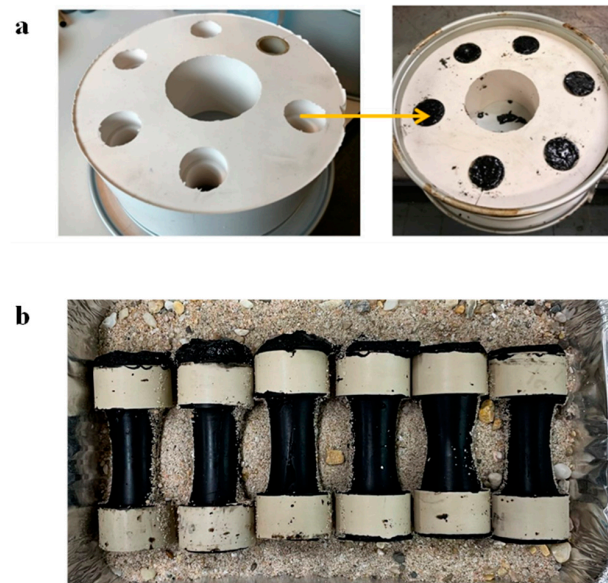


**Figure 3.** (a) The silicone mold containing the mortar, and (b) the demolded mortar sample.

**Table 4.** Properties of sand used in bituminous mortar.

Property	Source	Grain Size	Specific Gravity	Bulk Density	Moisture Content	Fineness Modulus	Gradation	Silt and Clay Content
Values	crushed sand	0.075 mm to 4.75 mm (ASTM C33 [33] Standard)	2.63 g/cm <sup>3</sup>	1.52 g/cm <sup>3</sup>	0.5%	2.6	Conforms to ASTM C33 specifications	<5%

Each mold allowed for the production of six specimens simultaneously, which were later stored horizontally in a sand-filled container upon removal from the mold, as depicted in Figure 3b. These specimens underwent meticulous inspection to detect any significant pores or defects.

Following preparation, the specimens underwent monotonic tensile testing. The mortar samples were loaded in tension using a Universal Testing Machine (UTM, IPC, Melbourne, Australia) at a controlled displacement speed of 0.1 mm/s at 5 °C and 20 °C. The specimen fixation during loading is illustrated in Figure 4.

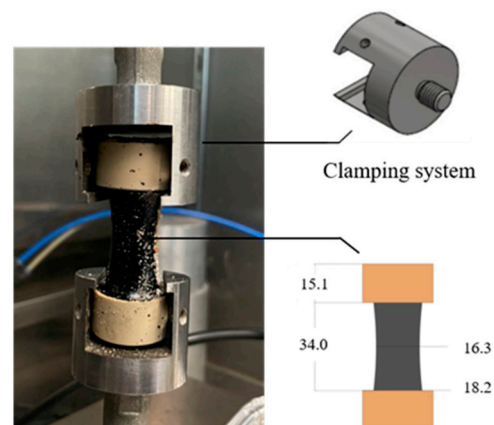


**Figure 4.** Tensile test setup.

This methodical approach ensured consistent specimen preparation, essential for accurately assessing how reed fibers affect the mechanical properties of bitumen mortar.

### 3. Results and Discussion

#### 3.1. FTIR

Figure 5a,b show the FTIR spectra of various samples, including virgin bitumen, modified bitumen with different amounts of reed fiber, and pure reed fiber. Key peaks observed in the FTIR spectra of reed fiber include the C-O stretch ( $1053\text{ cm}^{-1}$ ) and C-C stretch ( $1028\text{ cm}^{-1}$ ), which indicate cellulose deposition during secondary cell wall synthesis. Additionally, the  $\text{NH}_2$  peak ( $1537\text{ cm}^{-1}$ ) suggests the presence of proteins or amino acids, while the absorption peak at  $1633\text{ cm}^{-1}$  indicates adsorbed water—likely moisture from fiber storage—a hypothesis to be verified by testing dried fibers; further,  $-\text{CH}_2$  asymmetric stretching ( $2918\text{ cm}^{-1}$ ) and intermolecular hydrogen bonds ( $3334\text{ cm}^{-1}$ ) arise from waxes and cuticles on the fiber surface [34,35].

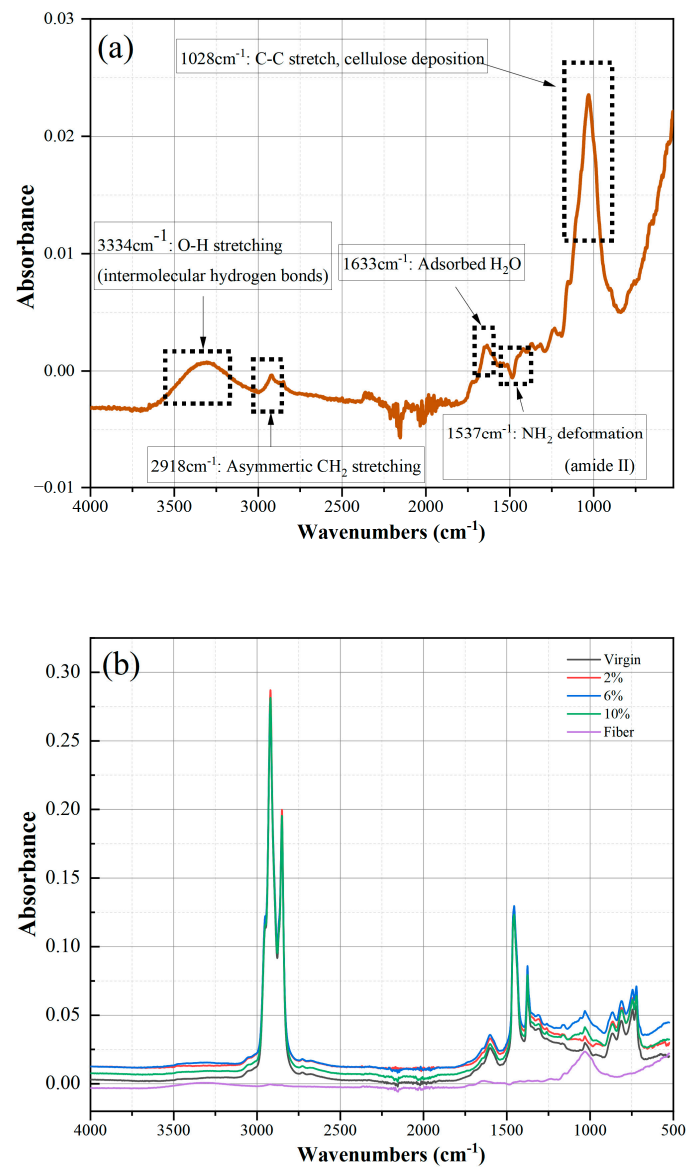


**Figure 5.** The FTIR spectra of (a) reed fiber, (b) virgin bitumen and RFBM.

In Figure 5b, it is apparent that the absorption peak intensities of modified bitumen and virgin bitumen are nearly identical, suggesting that the addition of reed fiber did not substantially alter the chemical composition of bitumen. This implies that the modification of bitumen with reed fiber involved physical mixing without significant chemical reactions. Furthermore, comparison of absorbance values between bitumen and fiber components reveals minimal absorption by the fibers. With a maximum fiber addition of 10%, the FTIR

spectrum of bitumen shows minimal interference from overlapping absorbance effects caused by the fibers.

A notable observation is the distinct absorption peak at  $1028\text{ cm}^{-1}$  in reed fiber, which shows an increasing trend in the peak area for 2%, 6%, and 10% RFMB. This observation could potentially serve as a criterion for evaluating the consistency of the fiber-bitumen blend in future research. It is important to note, however, that the iS50 FTIR Spectrometer manual specifies that infrared light used in the attenuated total reflection (ATR) test interacts only with the material's surface in contact with the ATR crystal, with penetration depths ranging from  $0.25$  to  $2.5\text{ }\mu\text{m}$  across the  $4000\text{--}400\text{ cm}^{-1}$  wavelength range [36]. Given the lower fiber content used in this study and potential limitations in fiber length, it is possible that few or no reed fibers make contact with the crystal during testing. Therefore, verification through transmission FTIR measurements may be necessary for future applications.

This refined explanation ensures clarity and coherence in describing the FTIR analysis and its implications for assessing the modification of bitumen with reed fiber.

### 3.2. Viscosity

In this study, eight test temperatures— $90\text{ }^{\circ}\text{C}$ ,  $100\text{ }^{\circ}\text{C}$ ,  $110\text{ }^{\circ}\text{C}$ ,  $120\text{ }^{\circ}\text{C}$ ,  $135\text{ }^{\circ}\text{C}$ ,  $150\text{ }^{\circ}\text{C}$ ,  $160\text{ }^{\circ}\text{C}$ , and  $170\text{ }^{\circ}\text{C}$ —were used to measure and plot the viscosity of RFMB to assess its temperature sensitivity. Figure 6 demonstrates that as temperature rises, the viscosity of RFMB decreases. Moreover, it shows an increase in viscosity with greater fiber length and dosage.

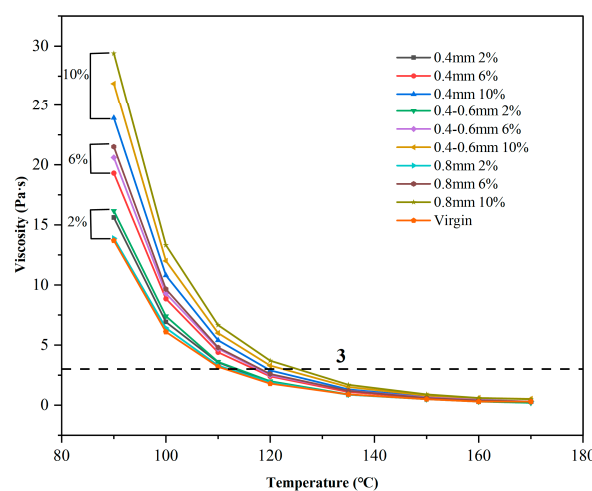


**Figure 6.** Viscosity varies with the temperature across each group.

Additionally, as depicted in Figure 6, the viscosity of RFMB shows a significant increase with higher fiber dosage, displaying three distinct gradients based on fiber content. Although fiber length also influences RFMB viscosity, even the longest fibers at a lower dosage exhibit lower viscosity compared to shorter fibers at a higher dosage. At lower fiber dosages, reed fibers primarily act as dispersing agents in bitumen, resulting in a limited viscosity increase. However, with increasing fiber dosage, reed fibers form a network structure, resulting in a viscosity increase of 1–2 times that of virgin bitumen. Importantly, all RFMB samples exhibit higher viscosity compared to virgin bitumen.

From a construction temperature perspective, RFMB requires sufficient heating during storage, blending, and pumping. Typically, after mixing, transporting, and pumping, the mixture is compacted around  $135\text{ }^{\circ}\text{C}$ . According to AASHTO standards, the viscosity of modified bitumen should not exceed  $3\text{ Pa}\cdot\text{s}$  at this temperature. Hence, bitumen with a viscosity below  $3\text{ Pa}\cdot\text{s}$  at  $135\text{ }^{\circ}\text{C}$  is deemed acceptable, with lower viscosity being preferable.

The viscosity–temperature relationship was utilized to determine the temperature at which each sample reaches a viscosity of  $3\text{ Pa}\cdot\text{s}$  at  $20\text{ rpm}$ , ensuring effective compaction in practical engineering, as depicted in Figure 7. The addition of reed fiber is observed to elevate the compaction temperature, consistent with the viscosity analysis discussed earlier.

Notably, the 0.8 mm fiber length at the 2% dosage exhibits a lower compaction temperature than samples with longer fibers at the same dosage, contrary to previous findings. This discrepancy might stem from difficulties in achieving uniform blending of longer fibers, resulting in a lower actual fiber dosage in the test samples.

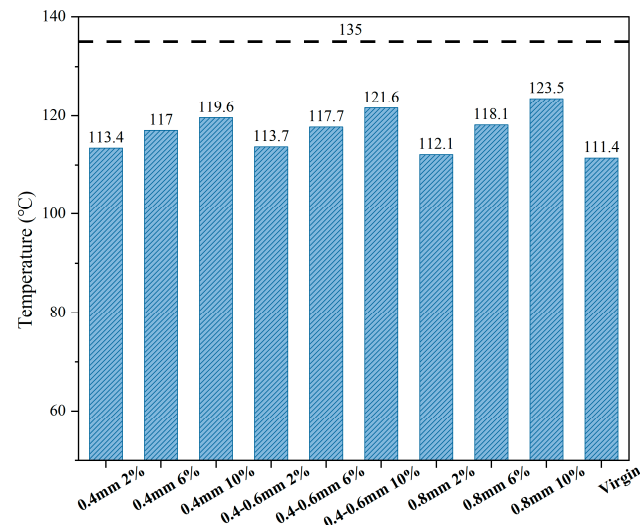


**Figure 7.** Temperature at 3 Pa·s viscosity for each sample at 20 rpm.

Additionally, Figure 8 shows viscosity measurements at 135 °C for each sample. While lower fiber dosages result in minimal changes in viscosity, higher dosages lead to a 50–80% increase, yet all samples meet the 3 Pa·s requirement, indicating that fiber addition does not compromise the bitumen's suitability for practical use. The similar viscosity values for 0.4 mm 2%, 0.4–0.6 mm 2%, 0.8 mm 2%, and virgin bitumen at 135 °C suggest that, under these conditions, variations in fiber length and dosage have a minimal impact on viscosity. This uniformity implies that at this temperature, the reed fibers' effect on the bitumen's viscosity is not pronounced, likely due to the high temperature mitigating the fibers' influence on the binder's flow properties.

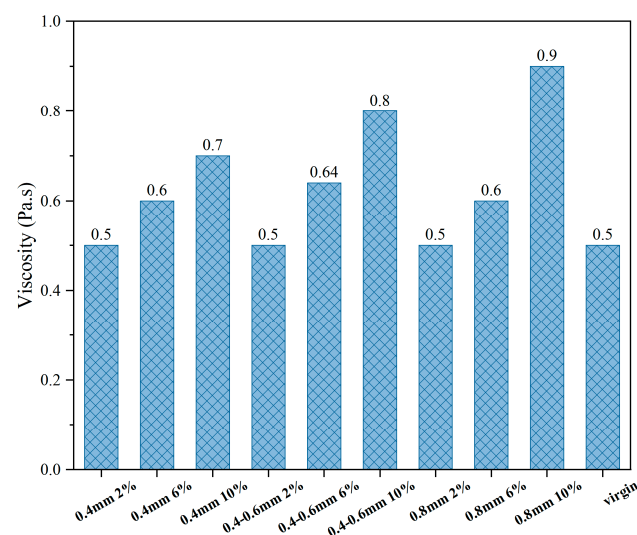


**Figure 8.** Viscosity at 135 °C.

This refined explanation provides clarity and coherence in discussing the impact of reed fiber on the viscosity and practical usability of modified bitumen in construction scenarios.



### 3.3. Frequency Sweep

Figure 9 depicts the relationship between the complex modulus of RFMB and loading frequency, highlighting how the modulus increases with the higher reed-fiber dosage in bitumen. Additionally, greater fiber length enhances the master curve of the complex modulus, though to a lesser degree than variations in fiber dosage, aligning with results from prior viscosity experiments.

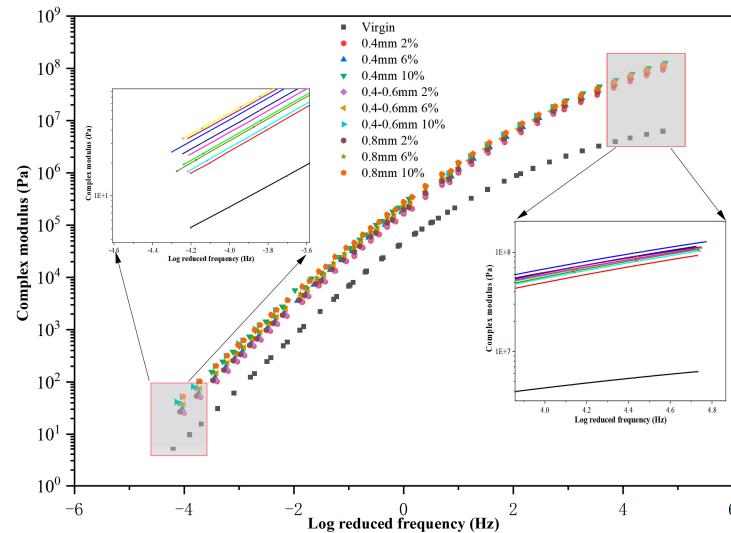


**Figure 9.** Complex modulus master curve at 30 °C.

The low-frequency region pertains to bitumen performance at high temperatures, whereas the high-frequency region reflects performance at low temperatures. Upon detailed examination of the frequency spectrum in Figure 9, it is evident that fiber addition markedly enhances the modulus across all temperatures compared to virgin bitumen. Notably, in the high-frequency range, the disparity between the RFMB and virgin bitumen curves is more pronounced, highlighting a substantial impact of reed fiber addition at higher frequencies. In RFMB groups, the modulus increases by approximately 100% at high temperatures, while the difference is around 10% at low temperatures, which is relatively insignificant. A higher  $G^*$  value indicates greater stiffness of the bitumen.

Here, the black space diagram is used to evaluate crack resistance, plotting the complex shear modulus  $G^*$  against phase angle  $\delta$  without relying on the time–temperature superposition principle. This diagram offers unique profiles for different types of bitumen. Anderson and colleagues introduced a method to fit the  $G^*$  master curve and phase angle using an essential parameter known as the R-value, as depicted in the following equation.

$$R = \frac{(\log 2) \times \log \frac{G^*(\omega)}{G_g}}{\log \left( 1 - \frac{\delta(\omega)}{90} \right)} \quad (2)$$

where  $G^*(\omega)$  is the complex modulus at frequency  $\omega$ ;  $G_g$  is the glassy modulus and assumed to be  $1 \times 10^9$  Pa;  $\delta(\omega)$  is the phase angle at frequency  $\omega$ . With the aid of the regions divided by the  $R = 1$ ,  $R = 2$ , and  $R = 3$  curves, it is interesting to view the results of modification on a black space diagram about potential damage, as shown in Figure 10.

The complex modulus at frequency  $\omega$  is denoted by  $G^*(\omega)$ , where  $G_g$  represents the glassy modulus assumed to be  $1 \times 10^9$  Pa and  $\delta(\omega)$  is the phase angle at frequency  $\omega$ . Divided into regions by the  $R = 1$ ,  $R = 2$ , and  $R = 3$  curves, the black space diagram provides insights into the impact of modification on potential damage, as depicted in Figure 10.

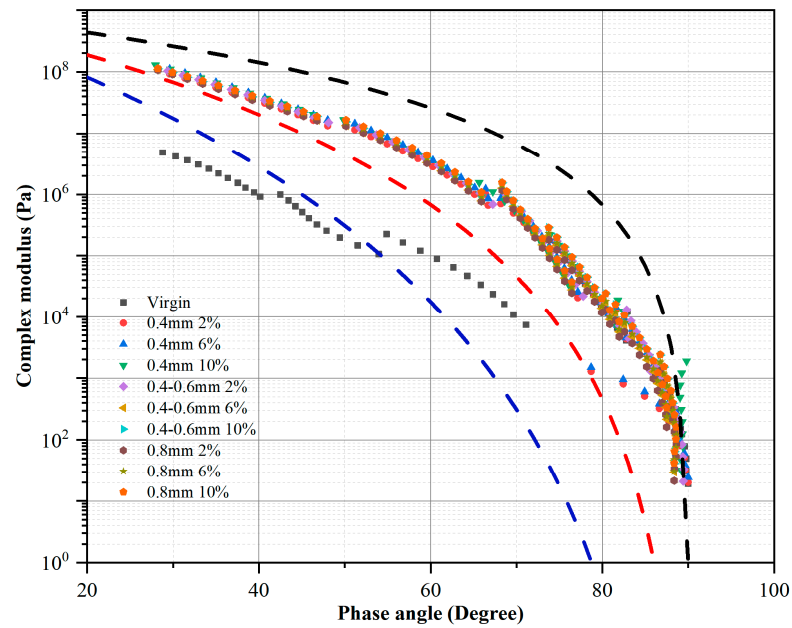


Figure 10. Black space diagram of rheological data.

Based on the R-value ranges, higher values indicate greater susceptibility to cracking. Areas in the lower-left corner of the graph signify potential for block cracking, while the upper-right corner indicates lower risk. Figure 10 illustrates that the addition of reed fiber shifts RFMB closer to curves associated with lower R-values compared to virgin bitumen, suggesting reduced susceptibility to cracking. This effect is particularly notable in the lower phase angle region, indicating improved resistance to low-temperature cracking due to fiber inclusion.

Conversely, among fiber-added groups, curves almost overlap, suggesting minimal distinguishable effects of fiber length and dosage on their mechanical properties.

This revised version maintains formality and coherence, offering a clear and precise discussion on how reed fiber influences the mechanical properties and crack resistance of bitumen.

### 3.4. MSCR

Figures 11 and 12 present the results from MSCR tests conducted at 70 °C and 76 °C.

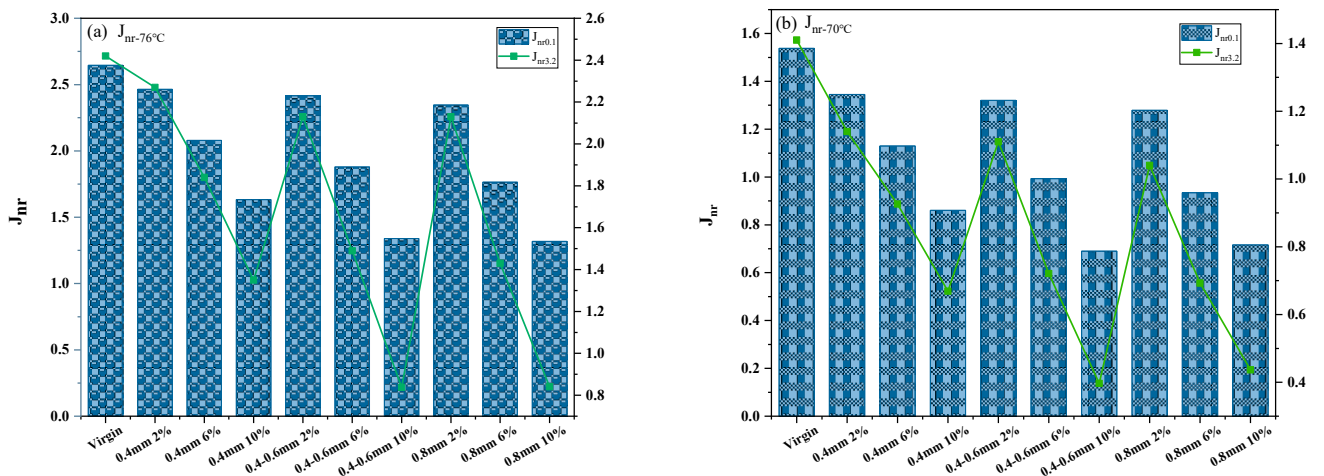


Figure 11.  $J_{nr}$  under (a) 76 °C and (b) 70 °C.

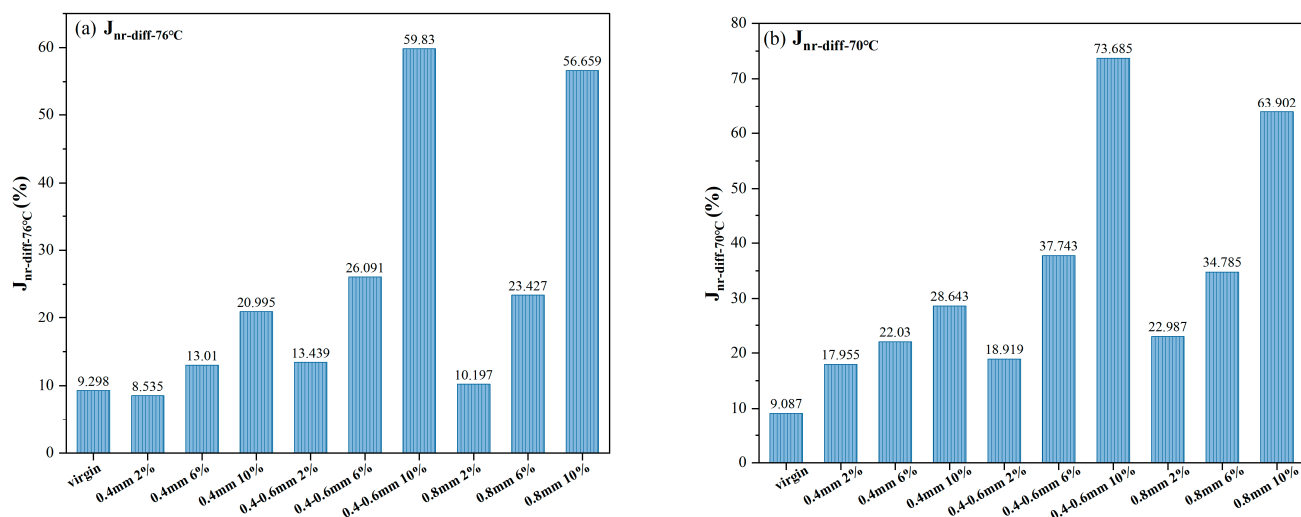


Figure 12.  $J_{nr-diff}$  under (a) 76 °C and (b) 70 °C.

In terms of  $J_{nr}$ , which signifies rutting resistance, all RFMB consistently exhibit lower values compared to virgin bitumen across both temperatures and stress levels. Notably, the value of  $J_{nr}$  decreases in an approximately linear manner with increasing reed fiber dosage, irrespective of variations in fiber length. Particularly, the RFMB containing 10% 0.4–0.6 mm reed fibers demonstrates superior rutting resistance under varied test conditions.

Conversely,  $J_{nr-diff}$ , indicating stress sensitivity, shows an increase with the addition of fiber. This trend opposes the observed improvement in rutting resistance. Higher fiber dosage, notably in the 10% 0.4 to 0.6 mm reed-fiber group, exhibits the highest stress sensitivity. This discrepancy is likely due to the aggregation of longer fibers at higher dosage levels, reducing their effectiveness and potentially acting as inert fillers within the bitumen matrix. This effect is less pronounced with 0.4 mm fibers.

According to AASHTO M332 [37] specifications, none of the modified bitumen samples exceeded the maximum allowable 75% limit for  $J_{nr-diff}$ . However, considering the variability in sample composition and blending conditions typical in practical applications, the elevated stress sensitivity observed in the 10% 0.4 to 0.6 mm reed-fiber group may limit its practical usability. Evaluating both rutting resistance and stress sensitivity collectively, the 6% 0.4 to 0.6 mm and 6% 0.8 mm modified bitumen samples exhibit superior rutting resistance and relatively lower stress sensitivity.

These findings highlight the intricate relationship between fiber dosage, length, and their impact on the mechanical properties of bitumen. They provide valuable insights for optimizing fiber-modified bitumen formulations tailored to enhance performance in bitumen engineering applications.

### 3.5. Relaxation Test

Figure 13 displays the stress–time curve for the 0.4 mm 6% reed fiber group. At lower temperatures, the relaxation test assesses stress generation and relaxation capabilities. Figure 14 presents the maximum shear stress of each sample under identical shear strain, with the initial maximum shear stress normalized to 100%. Figure 15 displays the times required for the stress to decrease to 50% (T50) and 10% (T10) of their initial values for each sample.

The data clearly indicate a substantial increase in shear stress with the addition of reed fibers, suggesting greater stiffness of the RFMB. This increased stiffness at low temperatures also implies increased brittleness.

From Figure 15, it is clear that the time required for stress to return to 50% remains largely unchanged for RFMB compared to virgin bitumen. However, for stress to return to 10%, RFMB exhibits approximately half the time compared to virgin bitumen. This improvement indicates that the incorporation of fibers enhances stress relaxation and reduces residual stresses, which is typical of viscoelastic materials. The elastic component rapidly releases

part of the stress upon removal of external force, while the viscous component gradually releases the remaining stress over time. The addition of reed fibers increases the viscosity of bitumen, facilitating easier release of residual stresses compared to virgin bitumen.

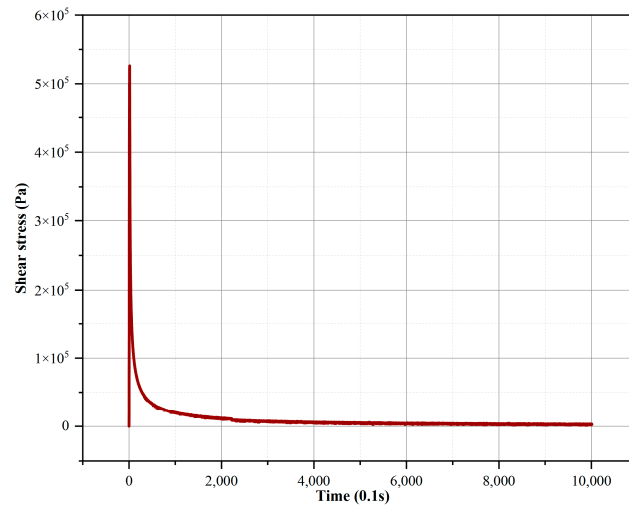


Figure 13. Stress–time relaxation curve for 0.4 mm and 6% reed fiber.

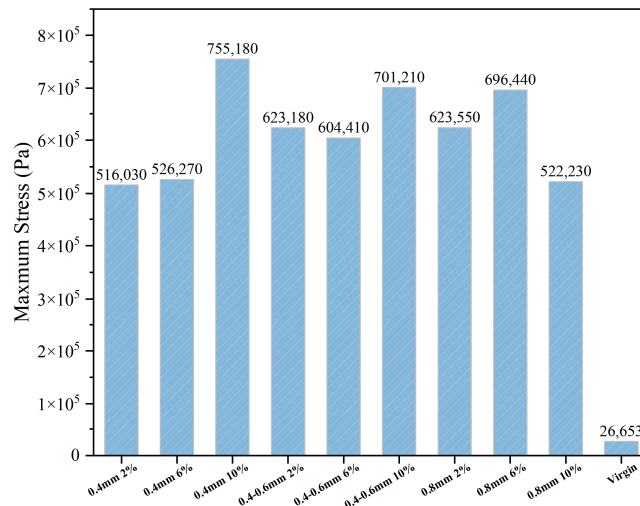


Figure 14. Maximum shear stress in relaxation testing.

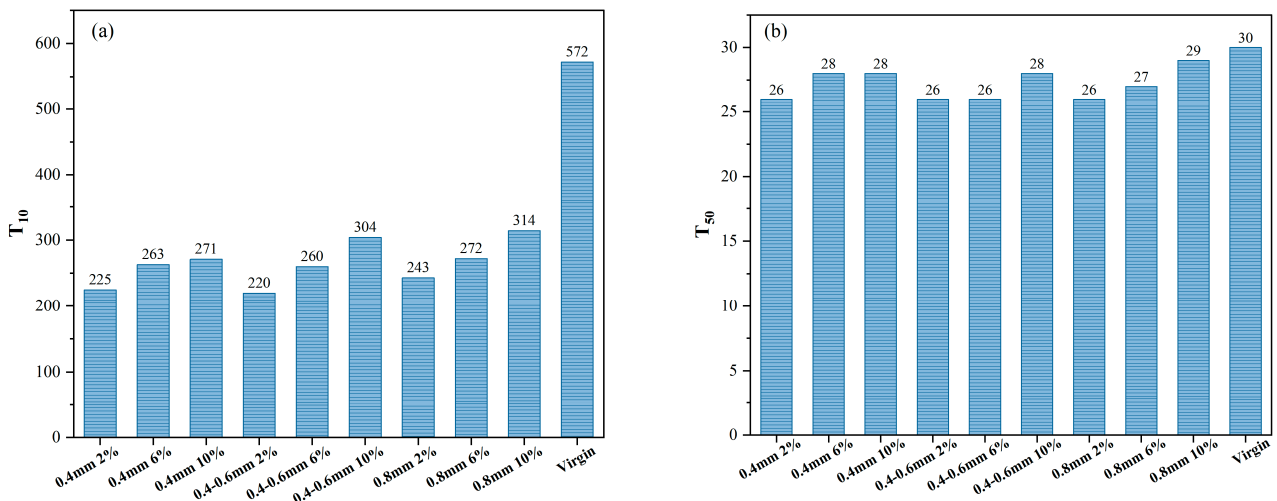


Figure 15. (a) Stress recovery time to 10% and (b) 50%.

Another consideration is the method employed for applying strain in DSR testing, where strain is induced by twisting the plate bonded to the bitumen, relying on the adhesion between the plate and the bitumen. The presence of fibers at this contact surface due to fiber addition may alter this adhesion, potentially reducing the ability of bitumen to maintain strain after application. This alteration could contribute to the observed stress relaxation behavior.

In summary, these findings underscore the complex interplay between fiber addition, material stiffness, stress relaxation, and adhesion dynamics in fiber-modified bitumen. They provide valuable insights into the viscoelastic properties and potential implications for bitumen engineering applications.

### 3.6. Linear Amplitude Sweep

Figure 16 displays the results of the linearly increasing amplitudes test. The area under the LAS curve, depicted in Figure 17, quantifies the energy required to fracture the samples. It is evident that with increasing shear strain, all RFMB samples show a distinct peak in shear stress, followed by a sharp decline, indicating sample damage.

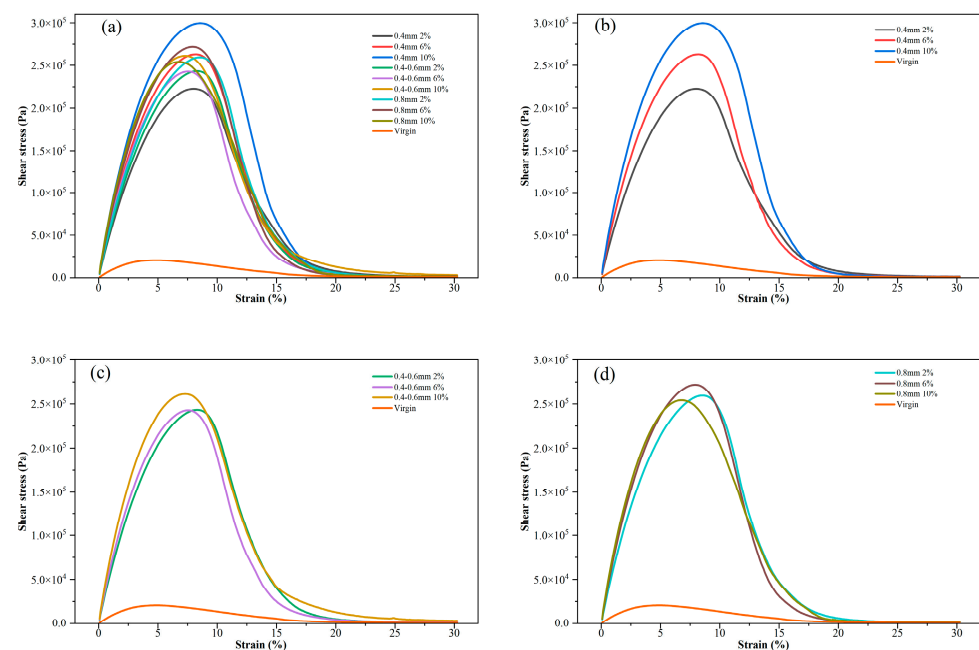


**Figure 16.** Stress–strain curves from LAS test with various reed fiber lengths: (a) all lengths; (b) 0.4 mm; (c) 0.4 to 0.6 mm; (d) 0.8 mm.

Specifically, in Figure 16a, the RFMB containing 0.4 mm reed fibers shows an increase in peak stress with higher fiber dosage, occurring at higher strain values. This suggests improved strain tolerance as the fiber dosage increases. This trend is less consistent across other fiber length groups but consistently shows peaks occurring beyond those of virgin bitumen. Similarly, Figure 16 indicates a comparable trend in the area under the LAS curve with increasing fiber dosage in the 0.4 mm and 0.8 mm groups. However, the influence of dosage variation in the 0.4–0.6 mm group is less pronounced, necessitating further investigation into its impact on enhancing bitumen strain tolerance.

Based on these results, the addition of 10% 0.4 mm reed fibers showed the most significant improvement in bitumen tensile strength. Using AASHTO TP 101-14, the fatigue performance parameter  $N_f$  was calculated from the aforementioned data and is depicted in Figure 18 for strain levels of 2.5% and 5%. RFMB demonstrated superior fatigue resistance across both strain levels, particularly with a 2% fiber addition across all fiber lengths. Specifically, at a 5% strain level and 2% fiber dosage, fatigue performance for 0.4 mm, 0.4–0.6 mm, and 0.8 mm reed fibers was 16.8, 17.2, and 17.4 times higher than that of virgin bitumen, respectively; however, at a 10% fiber dosage, these values decreased to 11.3, 7.7, and 6.5 times, respectively. Similar trends were observed at the 2.5% strain level, with



values of 13.0, 13.1, and 13.6 times higher at 2% dosage and 9.0, 6.5, and 5.4 times higher at 10% dosage.

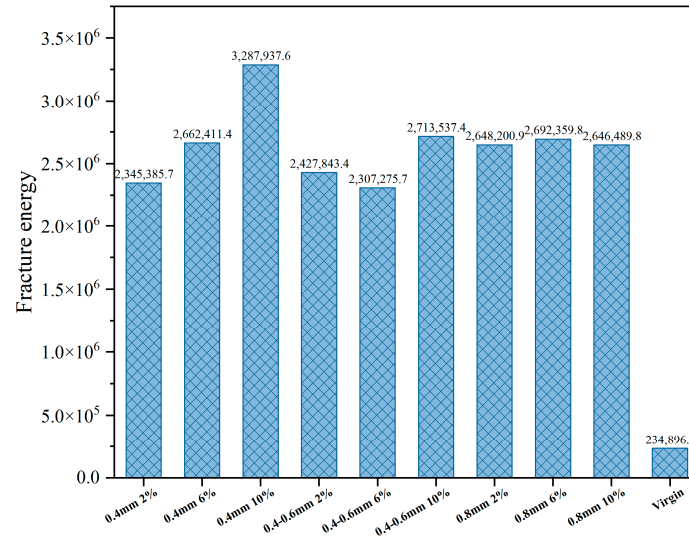


Figure 17. The area enclosed by the LAS curve.

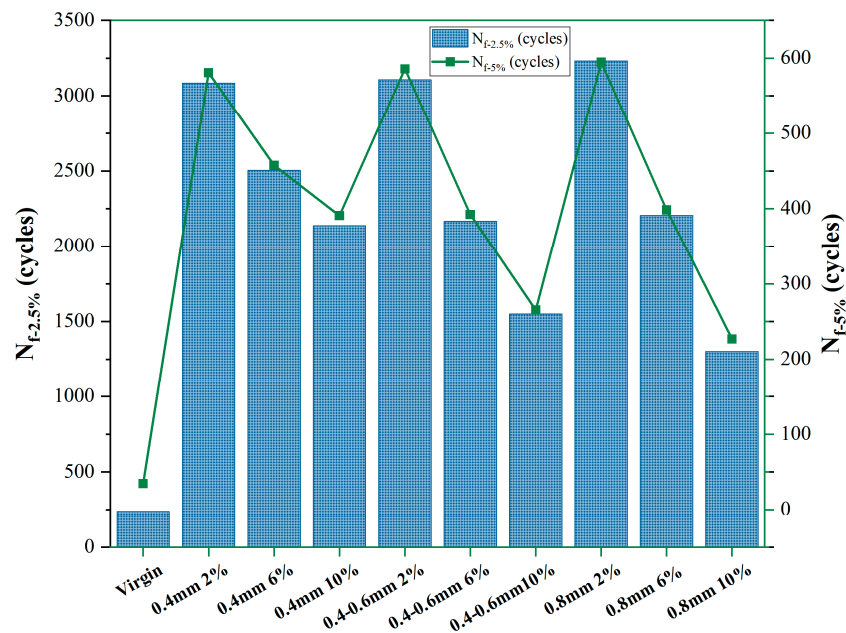


Figure 18. Predicted fatigue lives at 2.5% and 5% strain amplitudes.

Overall, the impact of fiber dosage was more pronounced in longer fiber lengths. Reed fibers significantly enhance fatigue resistance, with RFMB containing 0.8 mm fibers and a 2% addition exhibiting the most notable improvement in fatigue life.

The LAS test has recently played a crucial role in evaluating the damage tolerance of bitumen binders based on macrocrack growth rate trends [38]. Figure 19 depicts crack length ( $a_f$ ) calculated from the LAS test, representing the maximum allowable crack length before sample failure. Beyond this threshold, the crack length increases abruptly, indicating sample damage. Longer crack lengths at failure are preferable as they indicate greater tolerance to crack propagation [39].

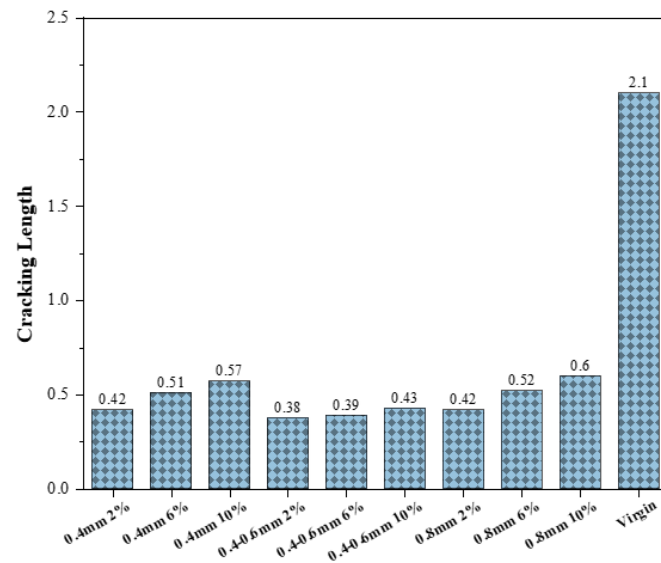


Figure 19. Crack length at failure.

### 3.7. Monotonic Tensile Testing of Mortar Reinforced with Reed Fibers

Figure 20 depicts the force–displacement data obtained from the monotonic tensile test, showing the maximum tensile force recorded for each specimen. Typically, the addition of fibers enhances the tensile strength of bituminous mortars [40]. Interestingly, when containing 6% reed fiber, the mortar showed the lowest strength among groups with similar fiber lengths, even demonstrating lower strength at 5 °C compared to the mortar without added fiber. The error bars suggest that the influence of fiber addition on tensile strength is not definitively clear. Nonetheless, at 20 °C, the addition of 2% 0.4–0.6 mm and 0.8 mm fibers showed significant increases of 3.09 and 2.59 times, respectively. This enhancement can be attributed to the reinforcing effect of fiber stiffness on the matrix, which is more pronounced at higher temperatures due to improved blending.

While higher fiber dosages enhance the ability to transfer forces between fibers within the specimen, the bond at the fiber–mastic interface remains the weakest link [41]. At elevated temperatures, the adhesion between fiber and mastic can surpass the cohesive strength of the mortar itself, which helps mitigate this weakness with higher fiber proportions. This accounts for the decrease in strength observed with 6% reed fiber at 20 °C, along with the slight increase with the 10% addition. In contrast, at 5 °C, there are no clear trends, and minimal differences between groups suggest that load transfer between fibers is less significant at lower temperatures. Nonetheless, the phenomenon of enhanced tensile strength with reed fiber addition remains uncertain and requires further investigation.

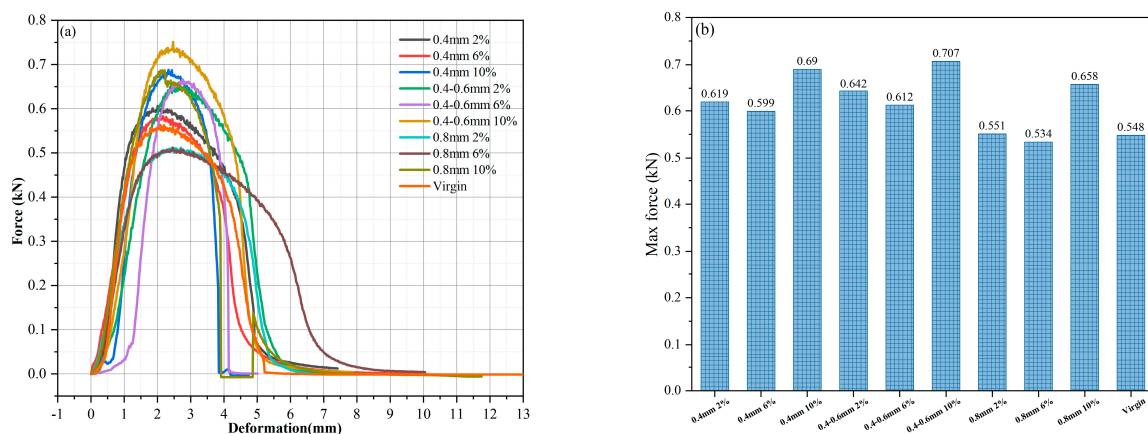
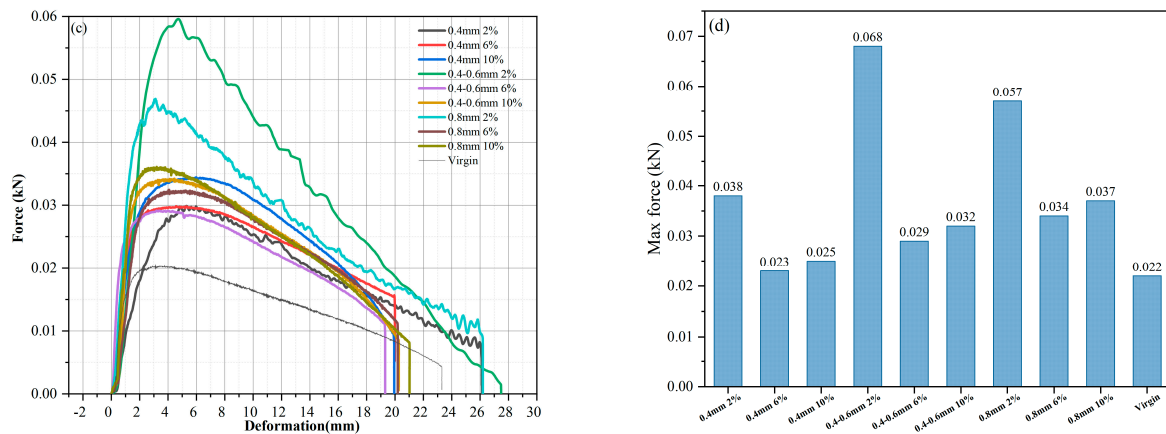
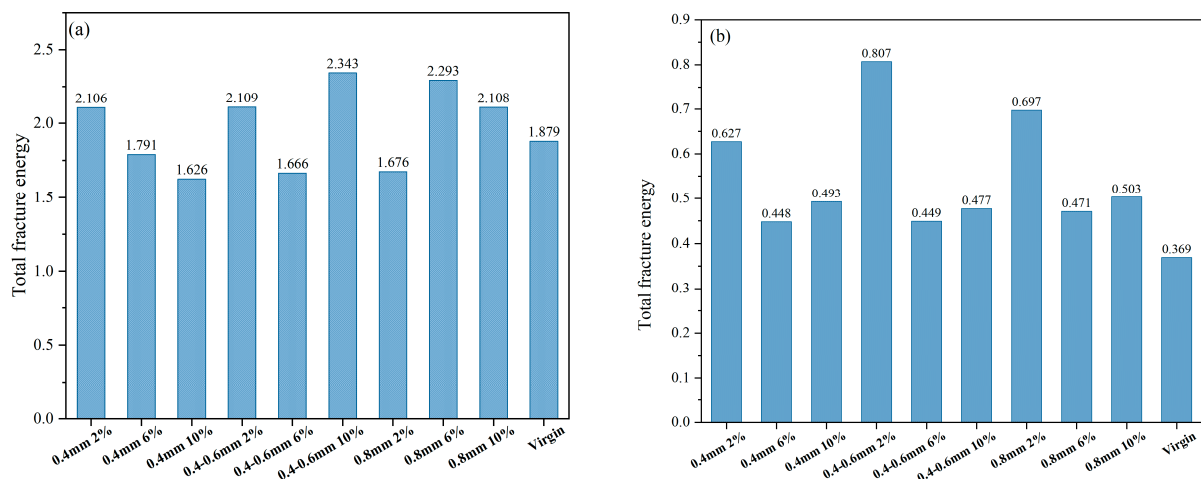


Figure 20. Cont.



**Figure 20.** (a) Force–deformation curve at 5 °C, (b) maximum tensile force at 5 °C, (c) force–deformation curve at 20 °C, (d) maximum tensile force at 20 °C.

Fracture energy, representing the material’s capacity to absorb energy before failure, is depicted in Figure 21 under monotonic tensile loading. At 5 °C, fibers did not significantly enhance the energy required to fracture the specimen, with irregular effects observed regarding fiber length and dosage. This inconsistency may arise from the interface zone between fibers and mastic becoming a potential weak point during low-temperature testing, which can accelerate specimen damage and reduce total energy absorption.



**Figure 21.** Fracture energy at (a) 5 °C and (b) 20 °C.

Conversely, at 20 °C, a notable enhancement in fracture energy was observed with 2% reed fiber dosage, while other fiber dosages did not show significant improvements, mirroring the strength analysis pattern. Notably, while 0.4 mm fibers exhibited considerable performance increases, the effect was slightly less pronounced than longer fibers, likely due to shorter fiber lengths limiting force transmission within the mastic.

In summary, the monotonic tensile test effectively demonstrated the enhancement in tensile strength afforded by reed fibers. Analysis based on peak forces indicates a more pronounced effect at 20 °C compared to 5 °C, highlighting the critical role of fiber–mastic adhesion at higher temperatures where fibers primarily contribute to mixture strength. The total fracture energy represents the stress and elongation of the specimen under tension, indicating the overall energy required to fracture the sample. Combining peak force and fracture energy data suggests that adding 2% of 0.4–0.6 mm reed fibers effectively enhances the tensile properties of the mortar.

### 3.8. Ranking

Based on the preceding tests, a straightforward ranking method is introduced to determine the optimal amount and length of fiber to incorporate. Each material is assigned a ranking value (RV) based on its performance across various tests, with the highest-performing material receiving an RV of 10 and the lowest-performing an RV of 1. The Total Ranking Value (TRV) for each material is then calculated by summing its RV across all tests. Table 5 summarizes the RV and TRV for both RFMB and virgin bitumen.

**Table 5.** Ranking values comparison between various RFMB and virgin bitumen.

Workability Parameters	0.4 mm 2%	0.4 mm 6%	0.4 mm 10%	0.4–0.6 mm 2%	0.4–0.6 mm 6%	0.4–0.6 mm 10%	0.8 mm 2%	0.8 mm 6%	0.8 mm 10%	Virgin
<b>Viscosity</b>	8	6	3	7	5	2	9	4	1	10
<b>High-Temperature Properties</b>										
$J_{nr 0.1}$	2	5	8	3	6	10	4	7	9	1
$J_{nr 3.2}$	2	5	8	3	6	10	4	7	9	1
$J_{nr diff}$	9	7	5	8	3	1	6	4	2	10
<b>Medium-Temperature Properties</b>										
LAS–Fracture energy	3	7	10	4	2	9	6	8	5	1
Fatigue life—5% strain	8	7	4	9	5	3	10	6	2	1
Fatigue life—2.5% strain	8	7	4	9	5	3	10	6	2	1
Cracking length at failure	3	6	8	1	2	5	4	7	9	10
<b>Low-Temperature Properties</b>										
Maximum stress	9	7	1	5	6	2	4	8	3	10
Relaxation(T10)	9	6	4	10	7	3	8	5	2	1
<b>Tensile strength of mortar</b>										
Tensile strength of mortar −5 °C	6	4	9	7	5	10	3	1	8	2
Tensile strength of mortar −20 °C	8	2	3	10	4	5	9	3	7	1
Fracture energy −5 °C	6	4	1	8	2	10	3	9	7	5
Fracture energy −20 °C	8	2	6	10	3	5	9	4	7	1
<b>Total ranking value</b>	<b>89</b>	<b>75</b>	<b>74</b>	<b>94</b>	<b>61</b>	<b>78</b>	<b>89</b>	<b>82</b>	<b>73</b>	<b>55</b>

The evaluated properties include performance across low, medium, and high temperatures, workability, and tensile strength of the mortar. Based on Figure 22, bitumen modified with 2% 0.4–0.6 mm reed fiber shows optimal overall performance. Additionally, the modified bitumen with reed fiber additions consistently outperforms virgin bitumen, indicating an overall enhancement in bitumen performance due to the addition of reed fibers. However, it should be noted that the bitumen modified with 10% fiber addition performs inadequately at low temperatures, suggesting that this level of fiber addition may not be suitable for applications in cold climates.

The ranking approach offers a structured method to assess different fiber types and quantities, facilitating the selection of the most effective reed fiber dosage and length to enhance bitumen properties.

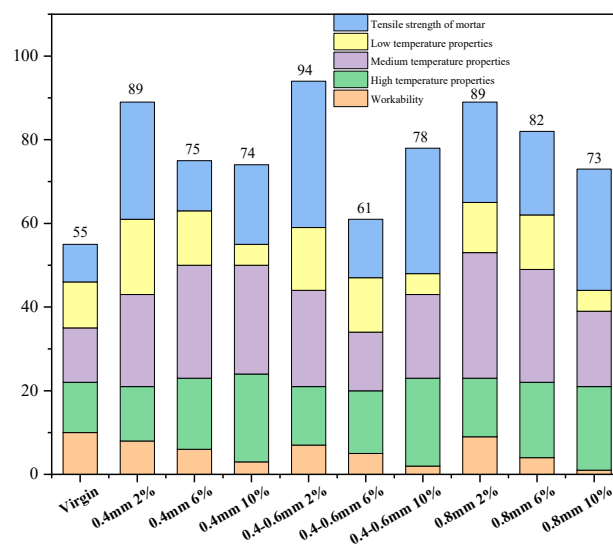


**Figure 22.** Rank values comparison: various RFMB and virgin bitumen.

#### 4. Conclusions

This paper investigates the modification of bitumen using reed fibers and examines their impact on bitumen properties across varying fiber lengths and dosages. This study encompasses comprehensive analyses, including the chemical characterization of RFMB, rheological evaluations of complex shear modulus and viscosity, tensile strength tests on mortar incorporating RFMB, and determination of optimal fiber length and dosage combinations. The key findings can be summarized as follows:

- 1 **Chemical Characterization:** FTIR analysis revealed that the addition of fibers did not alter the chemical structure of bitumen, confirming a purely physical blending process. Increased fiber dosage led to higher peak areas in RFMB spectra, particularly in the C-C stretch region of reed fibers, which serves as a criterion for determining optimal fiber dosage levels;
- 2 **Viscosity:** The viscosity of RFMB increased proportionally with higher fiber dosage. Longer fibers contributed to higher viscosity under equivalent dosage levels, although the effect was relatively minor, highlighting the role of fiber length in influencing viscosity;
- 3 **Rheological Tests:** Results from rheological tests indicated that adding reed fibers enhanced the complex shear modulus of bitumen, improving its performance at high temperatures; however, at low temperatures, higher fiber dosages exacerbated stiffness, indicating reduced flexibility. RFMB exhibited superior fatigue and rutting resistance but demonstrated poor stress sensitivity;
- 4 **Tensile Strength Tests:** Monotonic tensile tests on RFBM mortar showed varying effects of fiber addition. Significant improvements were observed primarily in mortars containing 0.4–0.6 mm and 0.8 mm fiber lengths. The shorter 0.4 mm fibers exhibited less pronounced reinforcement effects on bitumen, possibly due to uneven distribution during sample preparation, necessitating refinement in preparation methods for future studies;
- 5 **Ranking:** Based on the tests, bitumen modified with 2% of 0.4 to 0.6 mm reed fibers shows the best overall performance compared to other fiber dosages and types, consistently outperforming virgin bitumen. However, higher fiber dosages like 10% perform inadequately at low temperatures, indicating limitations in colder climates.

**Author Contributions:** H.C.: Methodology design, Data analysis, Writing-original draft. J.Z.: Data collection and analysis, Writing-original draft. D.N.: Supervision, Resources, Investigation, Validation. X.L.: Supervision, Methodology design, Writing—review and editing. P.L.: Methodology design, Data collection and analysis, Writing-original draft. All authors have read and agreed to the published version of the manuscript.

**Funding:** This work was supported by the Natural Science Basic Research Program of Shaanxi (No. 2024JC-YBMS-374), the Fundamental Research Funds for the Central Universities, CHD (No. 300102314902), the Shaanxi Housing and Urban–Rural Development Science and Technology (No. 2023-K12) and the Shaanxi Provincial Key R&D Program Projects (No. 2024GX-ZDCYL-03-09).

**Data Availability Statement:** Data are available with the first author and can be shared with anyone upon reasonable request.

**Conflicts of Interest:** Author Junyan Zhang was employed by the company Shaanxi Construction Engineering Eighth Construction Group Co., Ltd. The remaining authors declare that the research was conducted in the absence of any commercial or financial relationships that could be construed as a potential conflict of interest.

#### References

1. Chen, H.; Huang, S.; Niu, D.; Gao, Y.; Zhang, Z. Fatigue characterization and assessment methods for the terminal blend crumb rubber/SBS composite modified asphalt binders. *Constr. Build. Mater.* **2024**, *430*, 136357. [[CrossRef](#)]
2. Xu, J.; Liu, M.; Kang, A.; Wu, Z.; Kou, C.; Zhang, Y.; Xiao, P. Effect of fiber characteristic parameters on the synergistic action and mechanism of basalt fiber asphalt mortar. *Constr. Build. Mater.* **2024**, *438*, 137234. [[CrossRef](#)]
3. Li, H.; Liu, S.; Yang, F.; He, S.; Jing, H.; Zou, X.; Li, Z.; Sheng, Y. Review of utilization of bamboo fiber in asphalt modification: Insights into preparation, performance, reinforcement, and challenges. *J. Clean. Prod.* **2024**, *468*, 143010. [[CrossRef](#)]
4. Niu, D.; Zhang, Z.; Gao, Y.; Li, Y.; Yang, Z.; Niu, Y. Effect of pretreated cow dung fiber on rheological and fatigue properties of asphalt binder. *Cellulose* **2023**, *30*, 3773–3791. [[CrossRef](#)]



5. Morea, F.; Zerbino, R. Improvement of asphalt mixture performance with glass macro-fibers—ScienceDirect. *Constr. Build. Mater.* **2018**, *164*, 113–120. [[CrossRef](#)]
6. Zhao, H.; Li, G.; Ma, Y.; Yu, X.; Chen, Y.; Li, W. Long-term performance of chemically modified cotton straw fibers in micro-surfacing asphalt mixtures. *Case Stud. Constr. Mater.* **2024**, *20*, e03294. [[CrossRef](#)]
7. Gu, Y.; Li, H.; Wang, T.; Kong, J. Heat insulating properties of mullite hollow fibers prepared by using the template of reed fibers. *Open Ceram.* **2023**, *16*, 100490. [[CrossRef](#)]
8. Kbbing, J.; Thevs, N.; Zerbe, S. The utilisation of Reed (*Phragmites australis*)—A review. *Mires Peat* **2013**, *13*, 1–14.
9. Wang, X.; Deng, Y.; Wang, S.; Liao, C.; Meng, Y.; Pham, T. Nanoscale Characterization of Reed Stalk Fiber Cell Walls. *BioResources* **2013**, *8*, 1986–1996. [[CrossRef](#)]
10. Shon, C.S.; Mukashev, T.; Lee, D.; Zhang, D.; Kim, J.R. Can Common Reed Fiber Become an Effective Construction Material? Physical, Mechanical, and Thermal Properties of Mortar Mixture Containing Common Reed Fiber. *Sustainability* **2019**, *11*, 903. [[CrossRef](#)]
11. Bellatrache, Y.; Ziyani, L.; Dony, A.; Taki, M.; Haddadi, S. Effects of the addition of date palm fibers on the physical, rheological and thermal properties of bitumen. *Constr. Build. Mater.* **2020**, *239*, 117808. [[CrossRef](#)]
12. Chen, Z.; Yi, J.; Chen, Z.; Feng, D. Properties of asphalt binder modified by corn stalk fiber. *Constr. Build. Mater.* **2019**, *212*, 225–235. [[CrossRef](#)]
13. Fitzgerald, R. Novel Applications of Carbon Fiber for Hot Mix Asphalt Reinforcement and Carbon-Carbon Pre-Forms. 2000. Available online: <https://api.semanticscholar.org/CorpusID:138684383> (accessed on 29 August 2024).
14. ASTM D5/D5M-20; Standard Test Method for Penetration of Bituminous Materials. ASTM International: West Conshohocken, PA, USA, 2020. Available online: <https://www.astm.org/Standards/D5.htm> (accessed on 29 August 2024).
15. ASTM D36/D36M-14; Standard Test Method for Softening Point of Bitumen (Ring-and-Ball Apparatus). ASTM International: West Conshohocken, PA, USA, 2020. Available online: <https://www.astm.org/Standards/D36.htm> (accessed on 29 August 2024).
16. AASHTO T 316-2019; Standard Method of Test for Viscosity Determination of Asphalt Binder Using Rotational Viscometer. American Association of State Highway and Transportation Officials: Washington, DC, USA, 2019. Available online: <https://www.transportation.org> (accessed on 29 August 2024).
17. EN 15326:2007+A1:2009; Bitumen and Bituminous Binders—Measurement of Density and Specific Gravity—Capillary-Stoppered Pyknometer Method. European Committee for Standardization: Brussels, Belgium, 2009. Available online: <https://www.cen.eu> (accessed on 29 August 2024).
18. ASTM D4124; Standard Test Method for Separation of Asphalt into Four Fractions. ASTM International: West Conshohocken, PA, USA, 2020. Available online: <https://www.astm.org/Standards/D4124.htm> (accessed on 29 August 2024).
19. ASTM D7343; Standard Test Method for Determination of Viscosity of Asphalt Binder Using Rotational Viscometer. ASTM International: West Conshohocken, PA, USA, 2020. Available online: <https://www.astm.org/Standards/D7343.htm> (accessed on 29 August 2024).
20. AASHTO M320; Standard Specification for Performance-Graded Asphalt Binder. American Association of State Highway and Transportation Officials: Washington, DC, USA, 2020. Available online: <https://www.transportation.org> (accessed on 29 August 2024).
21. Xia, C.; Garcia, A.C.; Shi, S.Q.; Qiu, Y.; Warner, N.; Wu, Y.; Cai, L.; Rizvi, H.R.; D’Souza, N.A.; Nie, X. Hybrid boron nitride-natural fiber composites for enhanced thermal conductivity. *Sci. Rep.* **2016**, *6*, 34726. [[CrossRef](#)] [[PubMed](#)]
22. Wang, F.; Zou, G.; Xu, L.; Fan, S. Investigating the impact of calcium sulfate whisker on the microscopic properties of basalt fiber-reinforced asphalt using molecular dynamics simulation. *Constr. Build. Mater.* **2024**, *421*, 135643. [[CrossRef](#)]
23. Li, Z.; Guo, T.; Chen, Y.; Liu, J.; Ma, J.; Wang, J.; Jin, L. Study on pavement performance of cotton straw cellulose modified asphalt. *Mater. Res. Express* **2022**, *9*, 025508. [[CrossRef](#)]
24. Yashas, G.T.G.; Sanjay, M.R.; Parameswaranpillai, J.; Siengchin, S. Natural Fibers as Sustainable and Renewable Resource for Development of Eco-Friendly Composites: A Comprehensive Review. *Front. Mater.* **2019**, *6*, 226. [[CrossRef](#)]
25. ASTM E1252-98; Standard Practice for General Techniques for Obtaining Infrared Spectra for Qualitative Analysis. ASTM International: West Conshohocken, PA, USA, 1998. Available online: <https://www.astm.org/Standards/E1252.htm> (accessed on 29 August 2024).
26. ASTM D4402-14; Standard Test Method for Viscosity Determination of Asphalt at Elevated Temperatures Using a Rotational Viscometer. ASTM International: West Conshohocken, PA, USA, 2014. Available online: <https://www.astm.org/Standards/D4402.htm> (accessed on 29 August 2024).
27. Dong, W.; Ma, F.; Fu, Z.; Qin, W.; Qi, C.; He, J.; Li, C. Construction and examination of temperature master curve for asphalt with different aging extents. *Fuel* **2024**, *370*, 131819. [[CrossRef](#)]
28. ASTM D7175-15; Standard Test Method for Determining the Rheological Properties of Asphalt Binder Using a Dynamic Shear Rheometer (DSR). ASTM International: West Conshohocken, PA, USA, 2015. Available online: <https://www.astm.org/Standards/D7175.htm> (accessed on 29 August 2024).
29. ASTM D7405-15; Standard Test Method for Determining the Low-Temperature Performance Properties of Asphalt Binder Using Dynamic Shear Rheometer (DSR). ASTM International: West Conshohocken, PA, USA, 2015. Available online: <https://www.astm.org/Standards/D7405.htm> (accessed on 29 August 2024).

30. ASTM D7316-15; Standard Test Method for Determining the Elastic Recovery of Asphalt Binder Using a Dynamic Shear Rheometer (DSR). ASTM International: West Conshohocken, PA, USA, 2015. Available online: <https://www.astm.org/Standards/D7316.htm> (accessed on 29 August 2024).
31. Jiao, Y.; Du, W.; Yang, H.; Shi, H. Low temperature failure behavior analysis of fiber reinforced asphalt concrete under indirect tension test using acoustic emission and digital image correlation. *Case Stud. Constr. Mater.* **2024**, *20*, e02720. [[CrossRef](#)]
32. Tan, Z.; Leng, Z.; Li, H.; Ashish, P.K.; Cai, X.; Cao, P.; Sreeram, A. Quantitative analysis of asphalt concrete's tension-compression asymmetry effects on pavement response through 3D numerical modeling with dual viscoelastic model. *Constr. Build. Mater.* **2024**, *430*, 136427. [[CrossRef](#)]
33. ASTM C33; Standard Specification for Concrete Aggregates. ASTM International: West Conshohocken, PA, USA, 2022. Available online: <https://www.astm.org/Standards/C33.htm> (accessed on 29 August 2024).
34. Abidi, N.; Cabrales, L.; Hequet, E. Fourier transform infrared spectroscopic approach to the study of the secondary cell wall development in cotton fiber. *Cellulose* **2010**, *17*, 309–320. [[CrossRef](#)]
35. Zhang, X.; Zhao, H.; Li, C.; Wang, T.; Peng, L.; Li, Y.; Xiao, Y. In-situ micro-characteristics of fiber at the mortar transition zone in asphalt mixtures. *Constr. Build. Mater.* **2023**, *398*, 132529. [[CrossRef](#)]
36. Lee, L.C.; Liong, C.-Y.; Jemain, A.A. A contemporary review on Data Preprocessing (DP) practice strategy in ATR-FTIR spectrum. *Chemom. Intell. Lab. Syst.* **2017**, *163*, 64–75. [[CrossRef](#)]
37. AASHTO M332; Standard Specification for Performance-Graded Asphalt Binder Using Multiple Stress Creep Recovery (MSCR) Test. American Association of State Highway and Transportation Officials: Washington, DC, USA, 2021. Available online: <https://www.transportation.org> (accessed on 29 August 2024).
38. Zhang, Z.; Oeser, M. Understanding the damage mechanism of asphalt binder under controlled-stress fatigue loads in dynamic shear rheometer. *Constr. Build. Mater.* **2021**, *292*, 123463. [[CrossRef](#)]
39. Moraes, R.; Bahia, H.U. Effects of Curing and Oxidative Aging on Raveling in Emulsion Chip Seals. *Transp. Res. Rec.* **2018**, *2361*, 69–79. [[CrossRef](#)]
40. Xu, H.; Wu, S.; Chen, A.; Zou, Y. Influence of erosion factors (time, depths and environment) on induction heating asphalt concrete and its mechanism. *J. Clean. Prod.* **2022**, *363*, 132521. [[CrossRef](#)]
41. Yang, Q.; Fan, Z.; Yang, X.; Hao, L.; Lu, G.; Fini, E.H.; Wang, D. Recycling waste fiber-reinforced polymer composites for low-carbon asphalt concrete: The effects of recycled glass fibers on the durability of bituminous composites. *J. Clean. Prod.* **2023**, *423*, 138692. [[CrossRef](#)]

**Disclaimer/Publisher's Note:** The statements, opinions and data contained in all publications are solely those of the individual author(s) and contributor(s) and not of MDPI and/or the editor(s). MDPI and/or the editor(s) disclaim responsibility for any injury to people or property resulting from any ideas, methods, instructions or products referred to in the content.